Formation and Growth of a Nanosized RuIr Bimetallic Cluster Supported on NaY Zeolite

Sung June Cho* and Ryong Ryoo

Materials Chemistry Laboratory (School of Molecular Science, BK-21), Korea Advanced Institute of Science and Technology, Taeduk Science Town, Taejon 305-701, Korea

Received: June 27, 2000; In Final Form: November 27, 2000

A RuIr catalyst has been prepared by exchanging Ru and Ir metal ions simultaneously into NaY zeolite and then followed by thermal decomposition under a vacuum at 673 K and reduction with hydrogen at 623 K. The results obtained from the Xe adsorption measurement, hydrogen chemisorption, and X-ray absorption fine structure suggest that the RuIr bimetallic clusters are encapsulated in the supercage of NaY zeolite, consisting of 30−60 atoms/cluster. It has been found out that Ru and Ir atoms are homogeneously mixed in the bimetallic cluster. The nanosized RuIr bimetallic clusters in the NaY zeolite show strong resistance for the agglomeration in 1-atm oxygen and at high temperatures, compared to the Ru/NaY.

Introduction

Metal catalysts supported on NaY zeolite have been investigated extensively as model catalysts. The diameter of the supercage of the NaY zeolite is 1.3 nm and the pore aperture size is 0.7 nm, respectively, which is suitable for the formation of nanosized metal clusters.[1] Formation of bimetallic particles in the supercage of the NaY zeolite might offer better physicochemical properties, adsorption, catalytic performance, etc., compared to the corresponding monometallic catalysts.[2]

The RuIr bimetallic catalyst supported on alumina has been investigated due to its high activity for the N_2H_4 decomposition reaction.[3] Over the RuIr bimetallic catalyst, gasified N_2H_4 liquid is converted into gaseous N_2 and H_2 even at room temperature, resulting in the large volume increment, which can be utilized for satellite propulsion.

So far, it was not easy to form a 1-nm size RuIr bimetallic cluster inside the supercage due to different pretreatment conditions, thermal decomposition, and subsequent reduction for the Ru cluster and calcination and subsequent reduction for the Ir cluster, respectively.[4,5] There is controversy over the Ru mobility in NaY zeolite. Apple and Shoemaker reported that the Ru cluster was rather mobile under reducing conditions, while others suggested that the Ru cluster became volatile when it was subject to oxidizing conditions.[6] According to Shelef et al., the reduced metallic Ru transforms to RuO_2(s) and further RuO_3(g) or RuO_4(g) upon heating under oxidizing conditions.[7] The highly volatile RuO_3 and RuO_4 can be transformed into the perovskite-type ruthenate by adding BaO to lower the volatility. Cho et al. investigated extensively the redox behavior of the Ru cluster encapsulated in the supercage of Y zeolite using the Xe adsorption method, X-ray absorption fine structure (XAFS), and transmission electron microscopy.[4] They prepared the catalyst by ion exchanging $RuCl_3$ in aqueous NH_3 solution into NaY zeolite, followed by thermal decomposition and subsequent reduction. The *nano*sized reduced Ru cluster became agglomerated to form a bulk metal particle at the exterior surface of the zeolite crystal by heating at 573 K in 1-atm oxygen.

Recently, it became possible to prepare a 1-nm size Ir metal cluster in the supercage of NaY zeolite without calcination in O_2.[8] $IrCl_3$ was dissolved in aqueous NH_3 solution at 330 K for 24 h. The resulting Ir metal complex in the solution was found to be $Ir(NH_3)_5(H_2O)^{3+}$ from the curve fit of XAFS and elemental analysis. This Ir metal complex decomposed to form the reduced metal cluster at high temperature under vacuum in way similar to that for the Ru complex in NaY derived from $RuCl_3$ in NH_3(aq).[4]

In the present work, the nanosized RuIr bimetallic cluster supported on NaY zeolite is prepared by ion-exchanging Ru and Ir complexes into NaY zeolite in aqueous NH_3 solution. The catalyst was activated with the thermal decomposition and subsequent reduction by flowing hydrogen. The physicochemical properties of this RuIr bimetallic catalyst have been investigated using the Xe adsorption method, hydrogen chemisorption, Xe-129 NMR spectroscopy, and XAFS.

Experimental Section

$RuCl_3$ (Johnson Matthey, Ru 41.47%) and $IrCl_3$ (Johnson Matthey, 51.26%) was dissolved in concentrated aqueous NH_3 solution. The solution was heated at 330 K for 48 h with vigorous stirring. After the addition of NaY zeolite, $Na_{56}(AlO_2)_{56}(SiO_2)_{136}\cdot 250H_2O$, the solution was stirred for 72 h at 330 K. The zeolite sample was then filtered out, washed with deionized water, and dried in a vacuum oven at room temperature. The obtained zeolite sample was heated under 1×10^{-3} Pa while heated to 673 K with the ramping rate of 1 K·min^{-1} and maintained at 673 K for 2 h. Desorption of hydrogen from the catalyst was performed over 2 h at 673 K and 1×10^{-3} Pa. All the sample treatments were performed in situ in a Pyrex U-tube flow reactor connected to the NMR tube equipped with a homemade vertical ground-glass vacuum stopcocks. The NMR tube was sealed off with a flame after the sample was transferred to the tube. The total amount of Ru and Ir in the catalyst was 8 atoms/unit cell of zeolite and the Ir mol % was controlled to 0, 20, 40, 60, 80, and 100, respectively. The sample is designated as Ru_xIr_y/NaY, where x and y are the number of atoms per unit cell and their sum was controlled to 8. The metal contents of the catalyst were analyzed with the inductively coupled plasma

* To whom correspondence should be addressed. Present address: Catalytic Combustion Research Team, Korea Institute of Energy Research, 71-2, Jang-dong, Yusung-gu, Taejon 305-343, Korea. E-mail: sjcho@kier.re.kr. Fax: +82−420-860-3133.

10.1021/jp0022959 CCC: $20.00
Published on Web 01/27/2001

(ICP) atomic emission spectrometer (JY 38 Plus, Jobinyvon). The calculated and measured metal contents agreed well within 5% error.

Natural xenon gas (Matheson, 99.995%) was used for adsorption measurement as well as the Xe-129 NMR experiment. Xenon and hydrogen adsorption measurements were performed at 296 K with a conventional volumetric gas adsorption apparatus. The adsorption temperature was controlled to within 296 ± 0.1 K by a constant-temperature circulation bath.

Hydrogen chemisorption at 296 K was measured volumetrically after the preadsorbed hydrogen atoms were desorbed at 673 K in a vacuum (1×10^{-3} Pa) for 2 h and the sample cooled to 296 K. Extrapolation of this adsorption isotherm from 7 to 40 kPa to zero pressure was referred to as the total hydrogen chemisorption value, $(H/M)_{total}$. The sample was then evacuated at 296 K for 1 h, and a second isotherm was measured, which corresponded to reversible hydrogen chemisorption value, $(H/M)_{rev}$.

For the Xe-129 NMR experiment, the NMR tube containing the catalyst powder was in equilibrium with xenon at 296 K under given pressures. ^{129}Xe NMR spectra were obtained at 296 K with a Bruker AM 300 instrument operating at 83.0 MHz for ^{129}Xe with a 0.5-s relaxation delay. The chemical shift is referenced to xenon gas extrapolated to zero pressure.

For XAFS measurement, the catalyst precursor powder weighing 0.20 g was pressed into a self-supporting wafer of 10 mm in diameter. The wafer was treated with the same method as used above for the preparation of the RuIr catalyst in the Y zeolite supercage, using a Pyrex reactor. The sample wafer was transferred in situ into a joined EXAFS cell. Kapton (Du Pont, 125 μm) windows were glued to the EXAFS cell using Torr Seal (Varian) for the X-ray absorption measurement. The XAFS cell under H_2 atmosphere was sealed off with flame. The XAFS spectra were measured above both the Ru K edge and the Ir L_{III} and L_{II} edges by using beamline 10B at the Photon Factory in Tsukuba, Japan. A Si(311) channel cut was used to monochromatize the X-ray beam. The beam injection energy was 2.5 GeV, and the ring current was maintained as 300−350 mA. Incident and transmitted X-ray intensities were measured using ionization chambers filled with 100% Ar and 100% Kr for the Ru XAFS and 100% N_2 and 100% Ar for the Ir XAFS, respectively. The X-ray energies ($\Delta E/E = 1.0 \times 10^{-4}$) around the edge region and the EXAFS region increased in steps of 0.5 and 5 eV, respectively.

Results and Discussion

Formation of a Nanosized RuIr Bimetallic Cluster. The characterization of the nanosized bimetallic cluster supported on NaY zeolite has been performed using various methods, such as gas chemisorption, XRD, TEM, XAFS, etc.[9−11] We have measured the Xe adsorption and hydrogen chemisorption and Xe-129 NMR spectrum for the RuIr bimetallic catalyst. Table 1 lists the results of the sample characterization using the Xe adsorption method and hydrogen chemisroption. Ryoo et al. proposed the Xe adsorption method to estimate the number of atoms/cluster encapsulated in the supercage of Y zeolite.[9] A metal catalyst supported on faujasite type zeolite has been extensively investigated using the Xe adsorption method.[4,8−11] It is assumed that only four xenon atoms can be adsorbed on the metal cluster entrapped in the supercage of Y zeolite since only one xenon atom, 0.42 nm in diameter, can be direct contact with the metal cluster through the pore aperture, 0.70 nm. On the basis of this assumption, the average number of metal atoms/cluster can be obtained readily from the measurement of Xe adsorption on metal catalyst, *Xe/M*. The precision of the Xe adsorption method is found to be quite good while the accuracy depends much on the assumption made in the cluster size estimation.

TABLE 1: Hydrogen Chemisorption and Xe Adsorption on the RuIr/NaY

sample	$(H/M)_{total}$[a]	$(H/M)_{rev}$[b]	Xe/M ($\times 10^{-2}$)[c]	n[d]
Ir_8/NaY	1.59	0.42	0.66	61
$Ru_{1.6}Ir_{6.4}$/NaY	1.21	0.29	0.82	49
$Ru_{3.2}Ir_{4.8}$/NaY	1.09	0.27	0.86	46
$Ru_{4.8}Ir_{3.2}$/NaY	1.20	0.35	1.23	33
$Ru_{6.4}Ir_{1.6}$/NaY	0.90	0.33	1.19	33
Ru_8/NaY	0.90	0.41	1.20	32

[a,b] Measurement of hydrogen chemisorption at 296 K was carried out volumetrically after all the preadsorbed hydrogen was removed at 673 K and 1×10^{-3} Pa for 1 h and cooled to 296 K. A hydrogen chemisorption isotherm was obtained in the pressure range of 7−40 kPa at 296 K. Extrapolation of this isotherm to zero pressure gives total hydrogen chemisorption. The sample was then evacuated at 296 K and 1×10^{-3} Pa for 1 h and a new isotherm was measured. The extrapolation of the isotherm gave the reversible hydrogen chemisorption. [c] Two Xe adsorption isotherms were obtained volumetrically from each sample at 296 K. The first adsorption isotherm was obtained on the sample evacuated at 673 K. The adsorption temperature was controlled to within ±0.1 K by constant-temperature recirculation bath since the Xe adsorption was very sensitive to the temperature. Hydrogen or oxygen at approximately 1 atm was equilibrated with the sample. Hydrogen in the gas phase and the weakly adsorbed hydrogen were subsequently removed by evacuation for 30 min at 296 K. Then, the second isotherm was obtained. The difference between the extrapolation of the two Xe adsorption isotherms gave an amount of Xe adsorption on the metal cluster, where M is the total number of metal atoms in the sample. [d] Number of metal atoms per cluster is estimated assuming that only four Xe atoms can access to the cluster entrapped in the supercage of Y zeolite. Using $n = ZM/G$, where M is the total number of metal atoms, G is the amount of strong Xe adsorption on the cluster, and Z is the maximum number of Xe on the cluster, $\boldsymbol{n}$ can be calculated rigorously. The details of the calculation can be found elsewhere.[9]

For the Ru cluster entrapped in NaY zeolite, the number of atoms/cluster can be changed from 20 to 50 by varying the heating rate in the thermal decomposition and the temperature in the reduction.[4] The number of atoms/Ir cluster prepared from the $Ir(NH_3)_5Cl^{2+}$ was always around 50, referred from the results of XAFS, the Xe adsorption method, and hydrogen chemisorption.[5] However, recently Pak et al. reported a smaller Ir cluster consisting of 30 atoms prepared from $Ir(NH_3)_5(H_2O)^{3+}$ free of chloride.[8]

For the RuIr bimetallic catalyst, *Xe/M*, with *M* indicating Ru and Ir, varied from 0.120 to 0.066, corresponding to 30−60 atoms/cluster. The cluster estimated from the Xe adsorption method increased linearly with the Ir content. On the other hand, the results of the hydrogen chemisorption did not provide the detailed information of the cluster size below 1 nm with the Ir content because Ru and Ir seem to have a different hydrogen adsorption stoichiometry, 1 hydrogen/Ru and 2 hydrogens/Ir, respectively. For such a small RuIr cluster consisting of 30−60 atoms, the fraction of surface atoms in the cluster is almost close to unity. Thus, the hydrogen chemisorption can be insensitive for the change of the cluster size below or near 1 nm.

Xe-129 NMR spectroscopy explored by Fraissard is also a useful characterization method for the change of physicochemical environment in the supercage.[12] The interaction between the cluster or zeolite wall and Xe caused a large Xe-129 NMR chemical shift compared to that of free gaseous Xe. The formation and the growth of the Pt, Pd, Ir, Ru, and Rh clusters in the supercage can also be followed by Xe-129 NMR spectroscopy.[9] The large chemical shift from the RuIr bimetallic

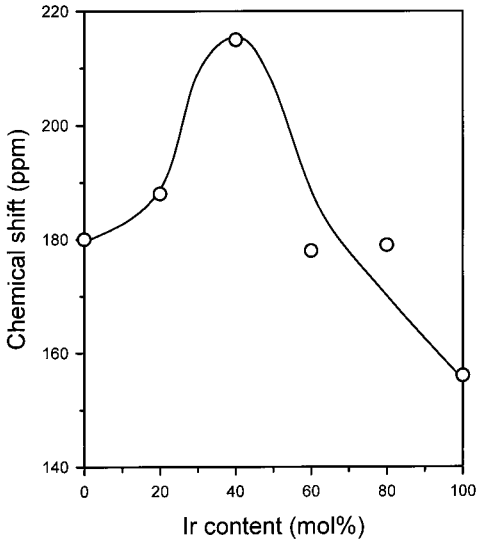

Figure 1. Dependence of the Xe-129 NMR chemical shift in the RuIr/NaY samples on the Ir content. The chemical shift was obtained at 53.3 kPa Xe gas and at 296 K.

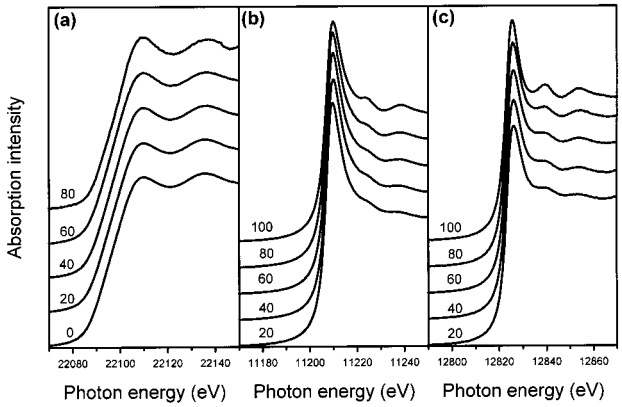

Figure 2. Near-edge structure of the X-ray absorption at the (a) Ru K edge, (b) Ir L_{III} edge, and (c) L_{II} edge. The number above the each line indicates the Ir content in mol %.

catalyst indicated the formation of a very small bimetallic cluster, because the interaction between the metal cluster in the supercage and Xe is strong. The heat of adsorption values of Xe, $\Delta H_{ads}/R = [\Delta \ln P/\Delta(1/T)]_{Ns}$, where Ns is the amount of Xe adsorption on the metal cluster obtained from the Pt cluster and Ru cluster on NaY, were -45 and -80 kJ mol^{-1}, respectively.[9] Ryoo et al. reported that such a Xe-129 NMR chemical shift of Xe adsorbed on the metal cluster in the supercage ranges widely from 500 to 3000 ppm depending on the type of metal and the size of the cluster.[9]

The chemical shift of Xe-129 NMR spectrum in Figure 1 shows the abnormal behavior depending on the content of Ir. The maximum chemical shift was obtained from the RuIr/NaY catalyst containing 40 mol % Ir at 215 ppm, which was larger than that of the monometallic Ru and Ir catalysts, 180 and 156 ppm, respectively. The large chemical shift due to the increased interaction between Xe and metal cluster may indicate the change of the surface electronic structure.

Figure 2 illustrates the near edge spectra of the bimetallic catalyst at the Ir L_{III} and L_{II} edge and Ru K edge. The structure at the X-ray absorption edge was indicative of the change of coordination geometry, oxidation state, etc.[13] Only a slight change in the near-edge spectra has been observed at the Ir L_{III} edge. The normalized maximum peak intensity decreased with the decrease of the Ru content, indicating an increase of the electron density in 5d orbital of Ir atom which is available for the dipole-allowed X-ray absorption transition, 2p $\rightarrow$ 5d. The second peak intensity also increased with the increase of Ir content, which can be attributed to either the change of the electronic structure like the extent of the d$-$sp hybridization or the increase of the cluster size. Meanwhile, there was negligible change in the near edge structure above the Ru K edge where the dipole forbidden transition, 1s $\rightarrow$ 4d, occurred.

Figure 3 show the k^3-weighted XAFS spectra and the corresponding Fourier transform at the Ru K edge and Ir L_{III} edge. The Fourier transforms of the Ru_xIr_y/NaY at both edges are also compared in Figure 4. There was a progressive change of Fourier transform intensity and the peak position as the increase of Ir content, indicating the formation of the Ru$-$Ir metallic bond. The curve fit was performed with XFIT[14] and FEFF6.01,[15] an ab initio XAFS program. The ranges Δk and Δr used for the curve fit were 30$-$130 and 0.15$-$0.30 nm^{-1}, respectively. The structural parameters were obtained from the iterative fitting using nonlinear least-squares method by optimizing the minimization function. The best fit of structural parameters is listed Table 2.

The Ru$-$Ir bimetallic bond distances at both edges are the same within the error range, $\pm$0.001 nm. All the coordination numbers in the bimetallic bond satisfied the criteria in the curve fit for coordination numbers of $N_{Ru-Ir}W_{Ru} = N_{Ir-Ru}W_{Ir}$ within a given error range.[16] With the increase of the Ir content, the Ir coordination increased progressively or vice versa, suggesting the formation of the homogeneously mixed bimetallic cluster. The total coordination number corresponded to cluster size approximately 1 nm or less to fit the supercage.

Surface Structure of Nanosized RuIr Bimetallic Clusters. The atomic structure referred from the XAFS results was a homogeneously mixed bimetallic cluster. Still, the microscopic surface composition of the cluster was not clarified. We noticed that the strong interaction between Xe and metal cluster can be inhibited due to the selective strong chemisorption of hydrogen or oxygen.[9] For the Ir metal cluster, hydrogen and oxygen play the same function to inhibit the Xe$-$metal interaction, while, for the Ru cluster, the chemisorption of hydrogen and oxygen cause different chemical shifts. There seems to be a substantial desorption of hydrogen from the Ru cluster in the evacuation after the chemisorption of hydrogen, letting Xe interact with the Ru cluster. The hydrogen-adsorbed Ru cluster showed a large chemical shift, 145 ppm, compared to that of oxygen-adsorbed Ru cluster, 100 ppm, as shown in Figure 5. Thereby, the surface composition of the cluster containing Ru can be studied using Xe-129 NMR spectroscopy combined with hydrogen chemisorption.

Figure 5 shows the dependence of the chemical shift on the Ir content with chemisorbed hydrogen and oxygen, respectively. It is intriguing that the chemical shift in the bimetallic RuIr cluster after the hydrogen chemisorption shows the linear dependence on the Ir content. It means that the composition of the surface structure is also proportional to the Ir and Ru content, consistent with the results of XAFS.

Agglomeration of Nanosized RuIr Bimetallic Cluster. The agglomeration of Ru metal clusters in Y zeolite has been studied because of the high mobility of Ru in hydrogen and oxygen,[6,17] which made the practical application of Ru catalyst difficult in the oxidizing and reducing conditions. Cho et al. showed that the agglomeration of Ru cluster in Y zeolite in hydrogen atmosphere was limited inside the supercage of Y zeolite while the agglomeration of Ru cluster in oxygen resulted in the

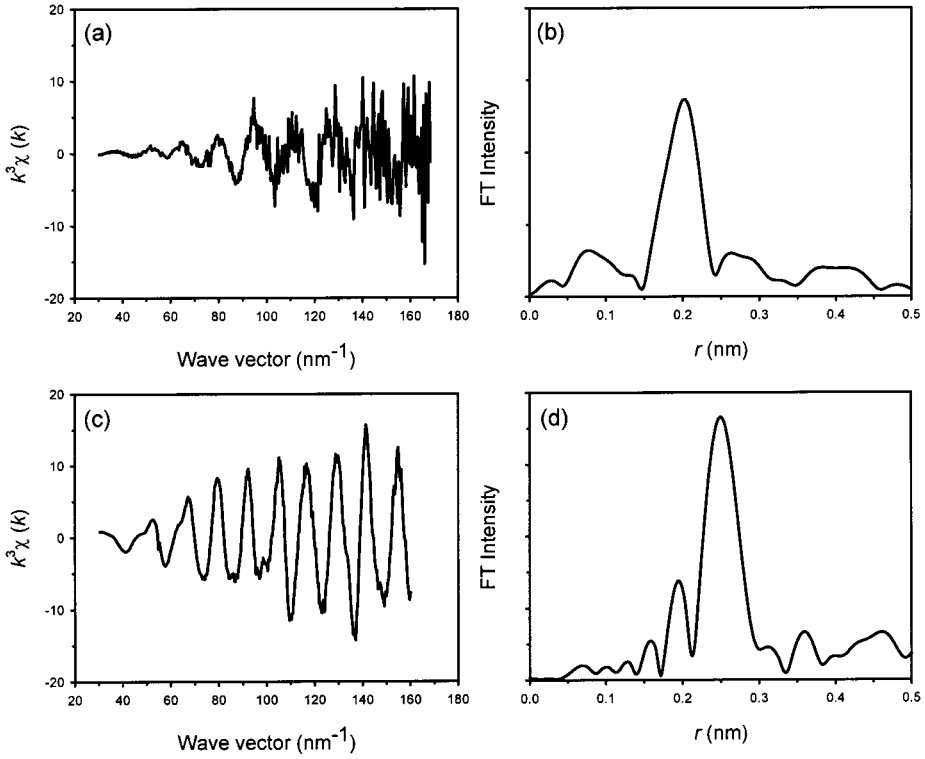

Figure 3. k^3-weighted XAFS spectra and those corresponding Fourier transforms at (a, b) the Ru K edge and (c, d) the Ir L_{III} edge.

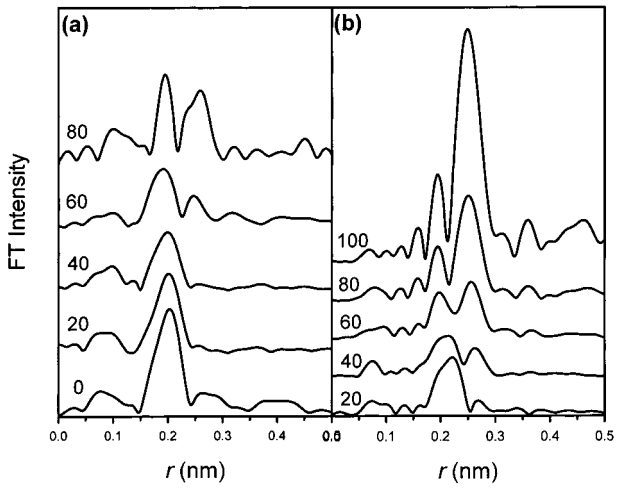

Figure 4. Phase shift uncorrected Fourier transforms of the sintered RuIr/NaY samples obtained above (a) the Ru K edge and (b) the Ir L_{III} edge. The number above the each line indicates the Ir content in mol %. The mismatch of the peak position with Table 2 is due to the phase shift.

formation of large agglomerates at the outer surface of the Y zeolite crystal.[4] The multivalent cations in the Y zeolite are known to stabilize Pt and Pd clusters inside the supercage.[18,19] For the Ru cluster inside the supercage of Y zeolite, the multivalent cations have little effect on the formation and the size of the cluster.[20] However, the agglomeration of Ru cluster in oxygen at the outer surface of zeolite crystal was suppressed using multivalent cations. The agglomeration process in oxygen can be monitored using Xe-129 NMR spectroscopy and XAFS. Also the redox behavior of ruthenium red complex or $Ir(NH_3)_5(H_2O)^{3+}$ in Y zeolite during the thermal decomposition was studied using Xe-129 NMR spectroscopy.[4,8]

Figure 6 shows the dependence of the chemical shift as a function of heating temperature in 1-atm oxygen. The progressive heating in oxygen led to a dramatic decrease of the chemical shift in the Ru cluster to 85 ppm at around 570 K. The chemical shift was the same as that of NaY under the same condition. Incorporation of Ir into the Ru cluster retarded the change of chemical shift to higher temperature, indicating the increase of the sintering resistance in oxygen. The retardation effect was proportional to the Ir content. The analysis of the Ru and Ir composition in the agglomerate was performed with XAFS. Figure 7 compares the Fourier transform for both Ru K- and Ir L_{III}-XAFS spectra. It was found from the Fourier transform that

TABLE 2: Structural Parameters for the RuIr/NaY Sample at the Ru K Edge and Ir L_{III} Edge

sample	atomic pair	N[a]	r (nm)[b]
Ir_8/NaY	Ir−Ir	7.9	0.269
$Ru_{1.6}Ir_{6.4}$/NaY	Ir−Ir	6.1	0.268
	Ir−Ru	1.2	0.265
	Ru−Ir	4.1	0.264
	Ru−Ru	1.0	0.261
$Ru_{3.2}Ir_{4.8}$/NaY	Ir−Ir	4.6	0.267
	Ir−Ru	1.3	0.264
	Ru−Ir	2.8	0.264
	Ru−Ru	2.7	0.261
$Ru_{4.8}Ir_{3.2}$/NaY	Ir−Ir	3.9	0.268
	Ir−Ru	2.3	0.264
	Ru−Ir	1.8	0.264
	Ru−Ru	2.9	0.261
$Ru_{6.4}Ir_{1.6}$/NaY	Ir−Ir	1.0	0.268
	Ir−Ru	3.4	0.265
	Ru−Ir	1.4	0.265
	Ru−Ru	4.7	0.260
Ru_8/NaY	Ru−Ru	6.0	0.257

[a,b] The XAFS data were collected in-situ at the Photon Factory, Tsukuba, Japan, using the BL-10B and BL-7C. The manybody reduction factor, S_0^2, used in the curve fit was 0.840 for Ru and 0.835 for Ir, respectively, which was obtained from the Ru and Ir references. The curve fit was done with nonlinear least-squares method, and the best fit was obtained by optimizing the minimization function. The Monte Carlo analysis of the estimated standard deviation including random noise in XAFS spectrum showed the reliable error range for $N \pm 0.1$ and $r \pm 0.001$

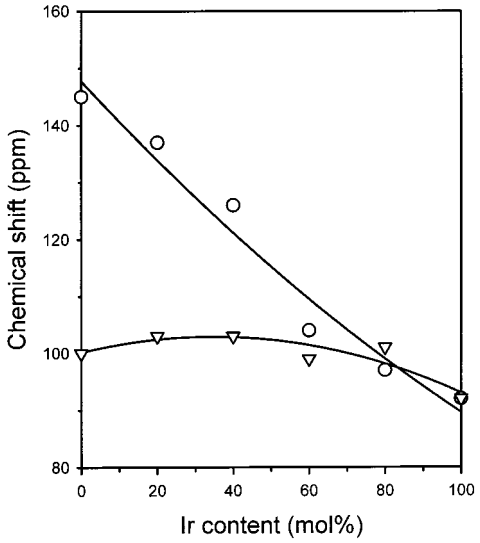

Figure 5. Dependence of the Xe-129 NMR chemical shift of the Xe adsorbed on the RuIr/NaY samples on the Ir content with (○) adsorbed hydrogen and (▽) adsorbed oxygen. The chemical shift was obtained at 53.3 kPa Xe gas and at 296 K.

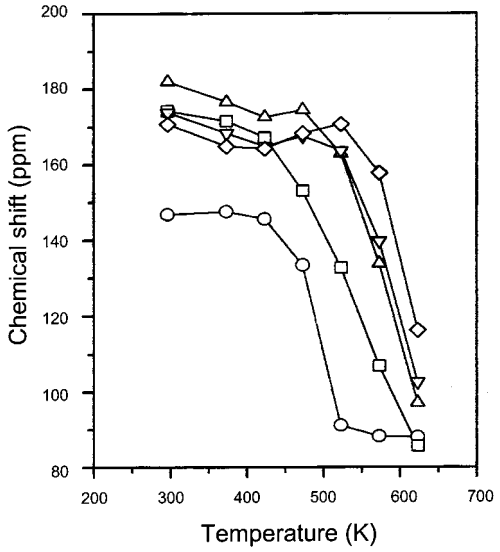

Figure 6. Xe-129 NMR chemical shift in the RuIr/NaY samples at 53.3 kPa Xe gas and 296 K plotted against the heating temperature under 1-atm oxygen: (○) 0 mol % Ir; (□) 20 mol % Ir; (△) 40 mol % Ir; (▽) 60 mol % Ir; (◇) 80 mol % Ir.

the sintering of the Ru cluster was suppressed with the incorporation of Ir. More quantitative information about the structural parameters is found in Table 3.

The structural parameters from the curve fit of XAFS did not satisfy all the necessary conditions for the bimetallic alloy, indicating the heterogeneous distribution of metal particles with the different Ru and Ir content. Both the monometallic clusters grew to bulk agglomerates upon heating in 1-atm oxygen. However, the formation of a bimetallic cluster dramatically suppressed the sintering with the increase of the Ir content, which can be considered as due to the effect of the bimetallic cluster. Interestingly, the contribution of the Ru−Ir bond in the $Ru_{6.4}Ir_{1.6}$/NaY sample at the Ru K edge was not detected whereas the Ir−Ru bond at the Ir L_{III} edge was detected. The similar structural parameters were also obtained from the $Ru_{4.8}$-$Ir_{3.2}$/NaY sample. These results were consistent with the formation of separate particles where the surface of the Ir cluster was covered partially with Ru. In this case, the contribution of

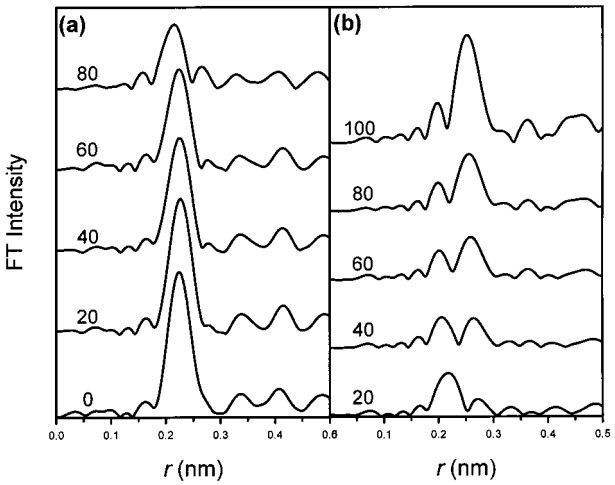

Figure 7. Phase shift uncorrected Fourier transforms of the sintered RuIr/NaY samples obtained above (a) the Ru K edge and (b) the Ir L_{III} edge. The sample was heated in 1-atm oxygen and at 673 K for 1 h. The number above the each line indicates the Ir content in mol %. The mismatch of the peak position with Table 3 is due to the phase shift.

TABLE 3: Structural Parameters for the RuIr/NaY Sample at the Ru K Edge and Ir L_{III} Edge after Heating in 1-atm Oxygen at 673 K

sample	atomic pair	N	*r* (nm)
Ir_8/NaY	Ir−Ir	11.5	0.271
$Ru_{1.6}Ir_{6.4}$/NaY	Ir−Ir	7.6	0.270
	Ir−Ru	1.1	0.270
	Ru−Ir	n.d.[a]	n.d.[a]
	Ru−Ru	10.7	0.267
$Ru_{3.2}Ir_{4.8}$/NaY	Ir−Ir	7.4	0.270
	Ir−Ru	1.8	0.269
	Ru−Ir	n.d.[a]	n.d.[a]
	Ru−Ru	9.5	0.266
$Ru_{4.8}Ir_{3.2}$/NaY	Ir−Ir	6.4	0.270
	Ir−Ru	2.5	0.268
	Ru−Ir	4.0	0.267
	Ru−Ru	5.9	0.266
$Ru_{6.4}Ir_{1.6}$/NaY	Ir−Ir	5.6	0.268
	Ir−Ru	3.1	0.268
	Ru−Ir	4.7	0.266
	Ru−Ru	5.5	0.267
Ru_8/NaY	Ru−Ru	12.0	0.267

[a] The inclusion of the Ru−Ir contribution in the curve fit of Ru K edge XAFS spectrum made no difference in the minimization function compared to the case that only single Ru−Ru contribution was considered. Further, the curve fit including the Ru−Ir contirbution gave physically unreliable structural parameters about the Ru−Ir bond. Thus, in this case, the Ru−Ir contribution was considered as *not detectable*.

the surface-attached Ru to the X-ray absorption at the Ru K edge became negligible compared to that of bulk Ru. Meanwhile, the higher content of Ir in the cluster led to unique bulk bimetallic agglomerates, which is under current investigation.

Summary

Nanosized RuIr bimetallic clusters consisting of 30−60 atoms can be obtained from the thermal decomposition and reduction with hydrogen of the precursor zeolite containing Ru complex and $Ir(NH_3)_5(H_2O)^{3+}$ free of chloride. The bimetallic composition of the cluster surface and the core was proportional to the Ir content, referred from the Xe-129 NMR spectrum with chemisorbed hydrogen and the data analysis of XAFS both at the Ru K and Ir L_{III} edges. The incorporation of Ir into the cluster inhibits the thermal sintering of the bimetallic cluster under 1-atm oxygen. This sintering reaction resulted in separate bulk Ir and Ru phases in the catalyst with the high Ru content.

References and Notes

(1) Jacobs, P. A. In *Metal Clusters in Catalysis*; Gates, B. C., Guczi, L., Knozinger, H., Eds.; Elsevier: Amsterdam, 1986; p 357. (b) Gates, B. C. *Chem. Rev.* **1995**, *95*, 511.

(2) Sinfelt, J. H. *Bimetallic Catalysts: Discoveries, Concepts and Applications*; John Wiley & Sons: New York, 1983.

(3) U.S. Patent No. 4,124,538 (1978).

(4) Cho, S. J.; Jung, S. M.; Shul, Y. G.; Ryoo, R. *J. Phys. Chem*. **1992**, *96*, 9922.

(5) Yang, O. B.; Woo, S. I.; Ryoo, R. *J. Catal*. **1992**, *137*, 357.

(6) Shoemaker, R.; Apple, T. *J. Phys. Chem.* **1987**, *91*, 424.

(7) Shelef, M.; Gandhi, H. S. *Platinum Met. Rev.* **1974**, *18*, 2.

(8) Pak, C.; Cho, S. J.; Lee, J. Y.; Ryoo, R. *J. Catal*. **1994**, *149*, 61.

(9) Ryoo, R.; Cho, S. J.; Pak, C.; Kim, J.-G.; Ihm, S.-K.; Lee, J. Y. *J. Am. Chem. Soc.* **1992**, *114*, 76.

(10) Kim, J.-G.; Ihm, S.-K.; Lee, J. Y.; Ryoo, R. *J. Phys. Chem*. **1991**, *95*, 8546.

(11) Ahn, D. H.; Lee, J. S.; Nomura, M.; Sachtler, W. M. H.; Moretti, G.; Woo, S. I.; Ryoo, R. *J. Catal.* **1992**, *133*, 191. (b) Ryoo, R.; Pak, C.; Cho, S. J. *Jpn. J. Appl. Phys*. **1993**, *32-2*, 475.

(12) Chen, Q. J.; Ito, T. Fraissard, J. *Zeolites* **1991**, *11*, 239.

(13) Moraweck, B.; Renouprez, A. J.; Hill, E. K.; Baudoing-Savois, R. *J. Phys. Chem.* **1993**, *97*, 4288. (b) Davis, R. J.; Landry, S. M.; Horsely, J. A.; Boudart, M. *Phys. Rev. B* **1989**, *39*, 10580.

(14) Ellis, P. J.; Freeman, H. C. *J. Synchrotron Radiat.* **1995**, *2*, 190. (b) Ellis, P. J. H.; Freeman, C.; Hitchman, M. A.; Reinen, D.; Wagner, B. *Inorg. Chem*. **1994**, *33*, 1249.

(15) Rehr, J. J.; Mustre de Leon, J.; Zabinsky, S. I.; Albers, R. C. *J. Am. Chem. Soc.* **1991**, *113*, 5135.

(16) Pak, C.; Ryoo, R. *Appl. Magn. Reson*. **1995**, *8*, 475.

(17) Verdonck, J. J.; Jacobs, D. A.; Genet, M.; Poncelet, G. *J. Chem. Soc., Faraday Trans. 1* **1980**, *76*, 403.

(18) Homeyer, S. T.; Sheu, L. L.; Zhang, Z.; Sachtler, W. M. H.; Balse, V. R.; Dumesic, J. A. *Appl. Catal.* **1990**, *64*, 225.

(19) Moller, K.; Bein, T. *J. Phys. Chem*. **1990**, *94*, 845.

(20) Cho, S. J.; Yie, J. E.; Ryoo, R. *Catal. Lett.* **2000**, in press.